

Effect of Green Corrosion Inhibition by *Prunus persica* on AISI 1018 Carbon Steel in 0.5M H₂SO₄

A. Rodríguez-Torres¹, O. Olivares-Xometl², M. G. Valladares-Cisneros^{3,*},
J. G. González-Rodríguez¹,

¹ Centro de Investigaciones en Ingeniería y Ciencias Aplicadas, Universidad Autónoma del Estado de Morelos, Ave. Universidad 1001, Chamilpa, C.P. 62209, Cuernavaca, Morelos, México.

² Facultad de Ingeniería Química, Benemérita Universidad Autónoma de Puebla, Av. San Claudio, Ciudad Universitaria. Col. San Manuel, Puebla 72570, Puebla, México

³ Facultad de Ciencias Químicas e Ingeniería, Universidad Autónoma del Estado de Morelos, Ave. Universidad 1001, Chamilpa, C.P. 62209, Cuernavaca, Morelos, México.

*E-mail: mg.valladares@uaem.mx

Received: 26 June 2017 / Accepted: 9 January 2018 / Published: 5 February 2018

The extract of *Prunus persica* (*P. persica*) leaves was studied as a green corrosion inhibitor (GCI) of AISI 1018 steel in 0.5 M H₂SO₄ at 25 °C. The corrosion inhibition efficiency (CIE) was established by the weight loss, potentiodynamic polarization curves (PPC) and electrochemistry impedance spectroscopy (EIS) techniques. The results showed that the IE was directly proportional to the inhibitor concentration, obtaining a maximum IE at 600 ppm (97 %) with a residence time of 6 h. The analysis of the electrochemical parameters from the polarizations curves confirmed that the *P. persica* extract behaved as a mixed-type GCI with cathodic predominance. The micrographs confirmed negligible damage on the steel surface when protected with the *P. persica* as GCI against the corrosive medium. The GC-MS analysis detected a high concentration of α -Tocopherol (vitamin E) and β -Sitosterol among the phytochemicals present in the *P. persica* extract. *Lactuca sativa* (*L. sativa*) and *Artemia salina* Leach (*A. salina*) were used as bioindicators of possible toxic effects exerted by the GCI, finding that the germination of seeds and radicle development of *L. sativa* were little affected (30 % of inhibition for hypocotile develop) by the *P. persica* extract at 600 ppm. However, the GCI turned to be harmless for the second bioindicator (*A. salina*).

Keywords: *Prunus persica*, Green corrosion inhibitor, AISI 1018 Carbon steel, *Artemia salina* and *Lactuca sativa*.

1. INTRODUCTION

The decrease in the corrosion rate offers many economic benefits that can stem from diminishing the dissolution of metallic compounds that are, in most cases, harmful to the environment

with a concomitant lifetime extension of pieces of equipment exposed to corrosive media [1, 2]. In the industry, the use of corrosion inhibitors (CIs) is considered as the most efficient method to reduce the corrosion rate of metallic materials [3-5]. The heterocyclic organic compounds and their derivatives have been successful as CIs, although their toxicity is an important disadvantage, for it limits their application due to environmental impact reasons [6, 7]. Some authors have mentioned the successful corrosion inhibition activity (CIA) exhibited by organic compounds, which frequently depends on the presence of functional groups in their chemical structure and electron pairs provided by heteroatoms such as N, O, P or S; these features and the presence of π electrons as double (aromatic rings) or triple carbon-carbon bonds enable these compounds to form favorable interactions with the metal surface [8, 9]; when these characteristics are present in the different compounds of a GCI, its inhibition performance is boosted significantly [10-12].

The current search, development and application of natural compounds, as GCIs with low or null toxicity and environmental impact are the qualities of interest to be found by different research groups around world. In this way, the research of natural products (NPs) represents an important part of our scientific culture and it is usually aimed at screening these products in the search of biological activity, however, a lot of pharmacology, medicine, biology, chemistry and applied engineering regarding these NPs is still to be learned. Their diverse structures have enriched the collection of known organic molecules and many NPs have turned out to be either useful molecules or leading compounds in different industries. These are some reasons to promote the studies of NPs as GCIs.

Different tissues of vegetable species have been studied such as flowers, fruits and fruit peels. For example, *Tagetes erecta* (marigold flower) flower extract was studied and reported to obtaining a 94.00 % of IE in the corrosion inhibition of mild steel in 0.5 M of H_2SO_4 using 1000 ppm of GCI. Lutein (**I**) was present in the flower extract of *T. erecta* and was attributed as the NP responsible of corrosion inhibition (CI) [13].

The ethanol extract of the *Opuntia eliator* fruit was studied as GCI of mild steal in sulfuric acid and reported that 500 ppm of *O. eliator* displayed a CIE of 85.00 % and mentioned that the ethanol extract contained Opuntinol (**II**) as NP and 50 ppm of Opuntinol offer 72.58 % of CIE for mild steel in 1.0 M H_2SO_4 [14]. The fruit peel of *Opuntia ficus-indica* (cactus pear) was investigated as GCI against 1018 steel in 0.5 M H_2SO_4 , reported that 1000 ppm displayed a CIE of 94.00 % [15].

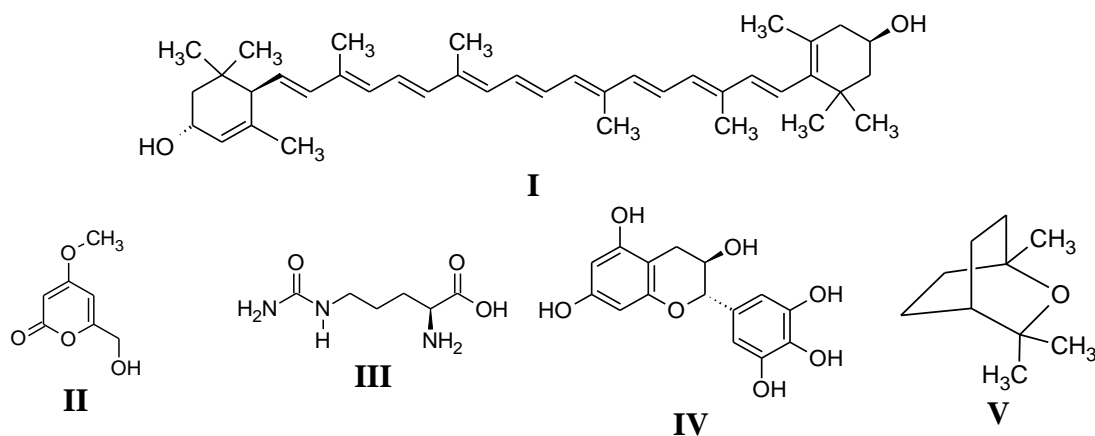


Figure 1A. Chemical structures of some natural products reported as GCIs

Watermelon peel was studied as GCI using mild steel in 1.0 M HCl and 0.5 M H₂SO₄, the authors reported that using 2000 ppm of watermelon peel extract producing a CIE of 81.00 % in HCl and 73.00 %, in H₂SO₄. In this study was mentioning that the CIA depended of the presence of L-Citrulline (**III**) [16]. Meanwhile, the CIA by *Mussa paradisiaca* (banana peel) extract by the use of mild steel in 1 M HCl at 26 °C. It was reported that 300 ppm of GCI yielded a CIE of 80.00 % and CIA was attributed to the presence of Gallocatechin (**IV**) in to the GCI [17].

In different studies, where plants have been used as CIs, it has been mentioned that the corrosion activity depends on the presence of flavonoids, alkaloids, and polyphenols; these compounds have in their molecular structures chemical characteristics to have a good corrosion inhibition performance [18-20]. Different authors have explained that corrosion inhibition occurs by the formation of an oxide layer on the metallic material that protects the surface against corrosion [21-23]. In this way the ethanol extract of *Hyptis suaveolens* leaves was studied as GCI and it was reported that it could inhibit efficiently the corrosion damage to produced by 1.0 M H₂SO₄ to carbon steel and found a maximum CIE of 95 % with the use of 250 ppm of GCI [24]. *Eucalyptus globulus* methanol extract was studied as GCI to protect carbon steel in 1.0 M H₂SO₄ and it was reported that the CIE increase with the concentration of GCI increased, finding that 1.5 gL⁻¹ of inhibitor gives a 85 % of CIE and mentioned that Eucalyptol (**V**) was the NP responsible of the inhibition [25].

In the same way, our interest is aimed at studying the corrosion inhibition capacity of *P. persica*, because it has been reported that peaches contain different bioactive compounds with antioxidant activity such as polyphenols and carotenoids [26-27], and both groups of NPs are good and harmless for the health [28].

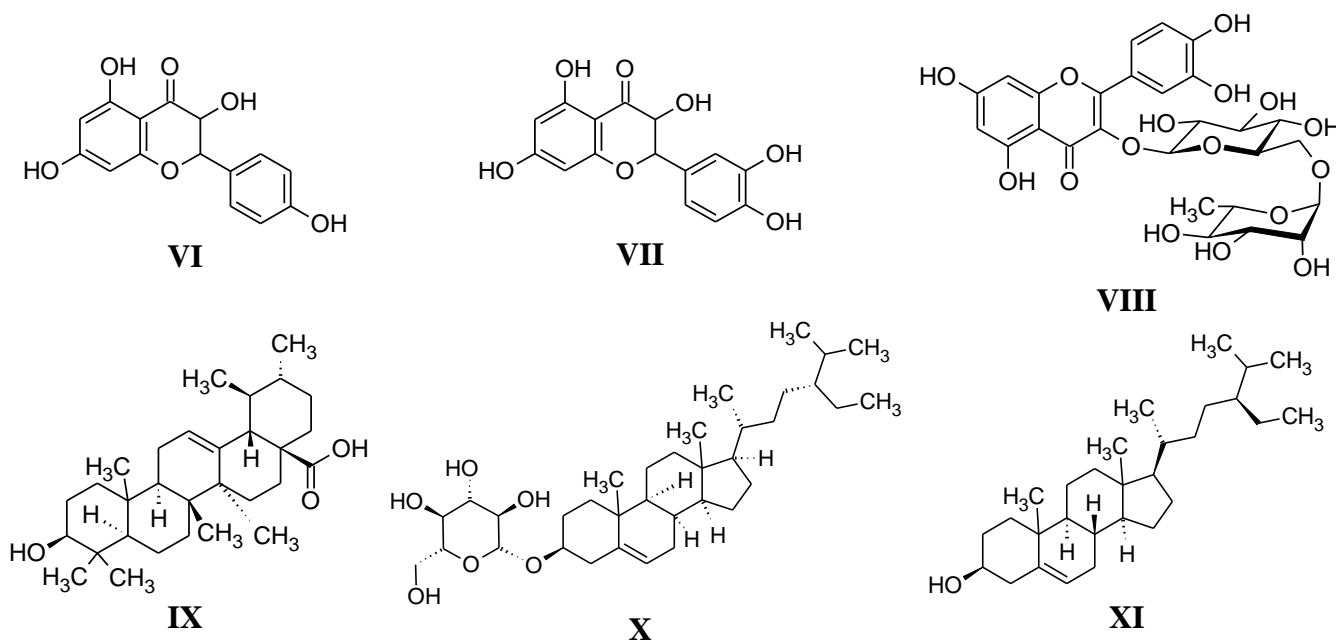


Figure 1B. Natural products isolated from *P. persica* and reported with antioxidant activity

P. persica (peach) is a tree from China, harvested from more than 4000 years ago, and currently, this specie is distributed in different parts of world [29]. Some phytochemical studies have mentioned that *P. persica* is rich in phenolic compounds (figure 1B) such as flavonoids, anthocyanins, procyanidins and hydroxycinnamic acids [30, 31].

In the *P. persica* leaves, flavonoids such as Kaempherol (VI), Quercetin (VII) and Rutin (VIII), and some terpenes such as Ursolic acid (IX), Daucosterol (X) and β -Sitosterol (XI) were identified [32-34].

The present study was aimed at studying the CI effect exerted by the extract of *P. persica* leaves on 1018 AISI Carbon steel in 0.5 M H₂SO₄ in order to contribute to increase the knowledge about the GCIs.

2. EXPERIMENTAL PROCEDURE

2.1 Metal specimen

Corrosion tests (weight loss) were carried out with AISI 1018 Carbon steel (C 0.14-0.20 %, Mn 0.60-0.90 %, P \leq 0.040%, S < 0.050 %, Fe balance, wt.%) coupons (2.5 cm x 0.6 cm). For the electrochemical tests, the coupons were embedded in epoxy resin having an exposure area of 0.36 cm². Before the tests, the coupons were abraded with wet SiC paper number 600; afterwards, they were washed with distilled water and degreased with acetone and stored in a desiccator for their further use. The surfaces of the blanks, in the presence and absence of GCI, were analyzed with a LEO 1450VP scanning electron microscope (SEM).

2.2 Green corrosion inhibitor (GCI)

P. persica leaves were recollected at the municipality of Huitzilac in the State of Morelos, Mexico. The leaves were dried at room temperature (25 °C \pm 2) for three weeks in a dark chamber with natural aeration. Afterwards, the leaves were finely cut (an average of 5 mm²) and exposed to a drying oven at 45 °C, under vacuum, for 72 h. The obtained material humidity was 20%. 500 g were macerated in a batch reactor with protection against ultraviolet light using 1 L of methanol (99 %) at 25 °C, atmospheric pressure and stirring rate of 50 rpm for 72 h. The obtained mixture was filtered and methanol was evaporated using a rotary evaporator, producing 65 g of *P. persica* extract and different concentrations of it in the ranged from 200 to 600 ppm were evaluated as GCI.

2.3 Aggressive solution

The test solution was prepared by using analytical grade H₂SO₄, which was diluted with deionized water to obtain a 0.5 M solution that was used to evaluate the properties of the *P. persica* extract as GCI of AISI 1018 Carbon steel.

2.4. Weight loss tests

The AISI 1018 Carbon steel coupons were immersed in 100 mL of 0.5 M H₂SO₄ in the absence and presence of different concentrations of *P. persica* extract for 6 h at 25, 40 and 60 °C. This temperature interval was selected because it is used in the industry during chemical pickling [35, 36]. All the tests were done in triplicate and the reported results represent the average of the performed tests. The corrosion rate (V_{corr}) was calculated by means of equation 1:

$$V_{corr} = \frac{534.W}{DAT} \quad (1)$$

where W is the weight loss (mg), D is density (g.cm⁻³), A is the specimen area (in²) and T is the exposure time (h).

The inhibition efficiency (IE_W , %) was calculated as follows:

$$IE_W, \% = \left[1 - \frac{V_{corr}}{V_{corr}^0} \right] \times 100 \quad (2)$$

where V_{corr}^0 and V_{corr} are the corrosion rates of iron samples obtained by weight loss with and without CI.

2.5. Electrochemical tests

The electrochemical measurements were carried out in a conventional three-electrode glass cell. A platinum counter electrode (99.99 % of purity) was used as auxiliary electrode and a saturated calomel reference electrode (SCE) via a Luggin capillary probe was used as the reference electrode. The working electrode was made of AISI 1018 Carbon steel. The electrochemical tests were performed in a potentiostat/galvanostat PGSTAT302N and the software Nova 2.0 was used to calculate electrochemical parameters. Before recording the data, the working electrode was immersed in the test solution until the steady-state open circuit potential (E_{OCP}) was reached (~15 min). The cathodic and anodic polarization curves were developed in the potential range from -250 mV to E_{OCP} , and from E_{OCP} to +250 mV at a scan rate of 1.0 mV s⁻¹. All the experiments were carried out thrice, and the reported data regarding the inhibition efficiency (IE_T , %) represent the average with a standard deviation of 0.3–3.5 %. equation 3 was used to calculate (IE_T , %):

$$IE_T, \% = \left[\frac{i_{corr1} - i_{corr2}}{i_{corr1}} \right] \times 100 \quad (3)$$

where i_{corr1} and i_{corr2} correspond to the current density value without and with inhibitor, respectively.

In the preliminary tests, the passive zone for this steel type in the absence of inhibitor was found at high anodic potentials. The EIS measurements were carried out in a PC4 300 Gamry

potentiostat, using an interval between 10 KHz and 0.5 Hz to obtain 50 points per decade at the E_{corr} value from the Stern-Geary equation [37,38].

2.6. Chemical analysis of the GCI

2.6.1. Fourier transform infrared spectroscopic analysis of the GCI

The chemical analysis of the *P. persica* extract was carried out by Fourier transform infrared spectroscopy (FTIR) using KBr pellets in a Bruker piece of equipment. The FTIR analysis was done by duplicate in order to detect the characteristic peaks of organic functional groups.

2.6.2. Gas chromatography coupled to mass spectrometry analysis of GCI

The *P. persica* extract was also analyzed by gas chromatography coupled with mass spectrometry (GC-MS) using a GC Agilent 6890 System Plus coupled with an Agilent 5973 Network Mass selective detector in order to detect the majority of organic natural compounds present in the green CI. The GC-MS is equipped with a silica capillary column (30 m X 0.25 mm of internal diameter and film thickness of 0.25 μ m). The GC conditions were 45-250°C using a gradient of 10 °C/min and injecting 1.0 μ L of *P. persica* extract at 0.02 g/L of concentration in methanol. The chemical compounds were separated through GC and were fragmented by MS. Each *P. persica* fragmentation spectrum was compared with the fragmentation index of the authentic pure compounds with the N-15598 database.

2.7. Bioassays of GCI

2.7.1 Lethality of *Artemia salina* Leach (brine shrimp)

The toxicity of the *P. persica* extract was evaluated by a lethality test using *A. salina* according to the procedure described by Meyer et al., (1982) [39]. Encysted eggs were purchased from the Aquatic Animal Research Center. Dried cysts were placed in a bottle containing artificial seawater, which was prepared by dissolving 35 g of sea salt in 1 L of distilled water. After 24-36 h of incubation at room temperature (28-30°C) under strong aeration and continuous illuminations conditions, the larvae (nauplii) hatched within 48 h. A stock solution of 100 mg of *P. persica* extract in 1 mL of distilled water was prepared. Seven fresh suspensions with different concentrations of green CI (fold serial dilutions) in artificial seawater were prepared immediately before use. 100 μ L of a suspension (at different concentrations of *P. persica* extract) were added to each well of 96-well microliter plates. After that, 10 nauplii in 100 μ L of artificial seawater per well were added to the 96-well plates and incubated at room temperature for 24 h. The numbers of surviving nauplii in each well were counted under a stereoscopic microscope after 24 h. The experiments were conducted in triplicate for each concentration. The negative control wells contained 10 nauplii and artificial seawater only. The death

percentages were calculated by comparing the number of survivors in the test and control wells [40]. The lethality was calculated by using Abbott's formula, equation 4:

$$\% \text{ lethality} = \left[\frac{\text{Test} - \text{Control}}{\text{Control}} \right] \times 100 \quad (4)$$

All the experiments were done in triplicate and the results represent the average with a standard deviation of 0.3–3.5 %. The *P. persica* extract toxicity was calculated from the 50% lethality concentration (LC₅₀) by means of Finney's Probit analysis [41].

2.7.2 Toxicity tests using *lactuca sativa* seeds

The *P. persica* extract was evaluated by acute toxicity against lettuce seeds (*Lactuca sativa* species) of a romaine variety, using the toxicity bioassay modified from Rodrigues-Da Silva Junior et al. [42]. The seeds of *L. sativa* (fungicide and pesticide free) were acquired from the Hortaflo brand. Ten lettuce seeds were exposed on filter papers impregnated with different concentrations of *P. persica* extract in the range from 0 to 1000 ppm, previously put in the Petri dishes (10 cm in diameter). Each concentration was assayed in triplicate and put in a plastic bag to preserve humidity. The negative control was mineral water solution and the positive control was a 0.02 M CuSO₄ solution. The dishes were incubated in the dark at constant temperature (24 ± 2 °C) for 120 h. After five days of exposure, the germinated seeds in each dish were counted and the radicle length and hypocotyl were measured and compared with the control. Analysis of the data was performed by means of Finney's Probit analysis [41].

3. RESULTS AND DISCUSSION

3.1. Weight loss tests

The concentration effect exerted by the *P. persica* extract as GCI on AISI 1018 Carbon steel in 0.5 M H₂SO₄ was analyzed by weight loss tests at different temperatures. The figure 2 shows that at the lowest GCI concentration (200 ppm) and 25, 40 and 60 °C, the highest *IE_W* were obtained (33, 20 and 18 %) whereas at the highest GCI concentration (600 ppm), the highest *IE_W* were of 80, 38 and 34 %. Nonetheless, as *IE_W* is inversely proportional to *V_{corr}*, it can be elicited from figure 2 that *V_{corr}* increases with the temperature, where the highest weight loss occurred at 60 °C; this phenomenon is associated with the decomposition or degradation of the *P. persica* extract as GCI.

In table 1, the *V_{corr}* and *IE_W* values are reported, where it can be observed that at 25 °C, the best *IE_W* percentages were obtained at the evaluated CI concentrations. However, at 40 and 60 °C, a slight increase in *IE_W* can also be appreciated. The *IE_W* behavior is due to a higher amount of *P. persica* extract molecules in the corrosive medium; for this reason, a higher number of active sites are protected, reducing the steel mass loss. The protection of the active sites occurs because the *P. persica* extract molecules possess functional groups and elements with a rich electronic density (figure 1B) in

their chemical structure, which facilitated the adsorption on the steel surface. The fact that the *P. persica* extract is more efficient as GCI at 25 °C is because its active compounds do not suffer degradation as it possibly occurred at 60 °C. Then, at 25 °C, the molecule/metal interactions are more stable on the active sites whereas at 40 and 60 °C, the inhibitor/metal adsorption phenomena are affected by changes in the activation energy promoted by the temperature effect [43].

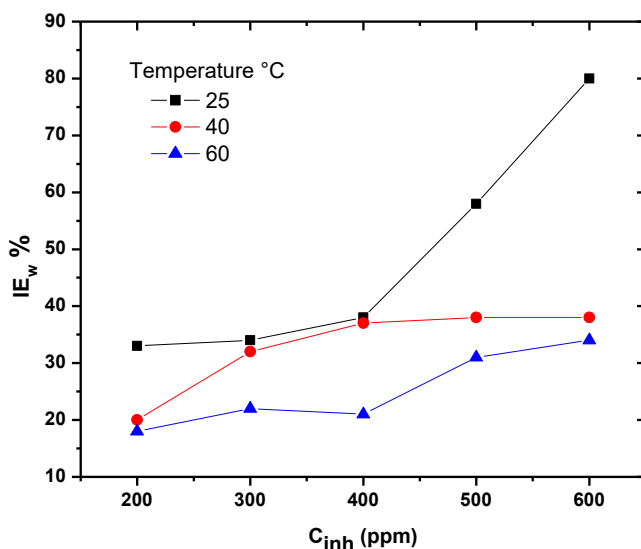


Figure 2. Effect of *P. persica* concentration and temperature on the CIE on AISI 1018 Carbon steel in 0.5 M H₂SO₄

In order to understand the adsorption phenomena of GCI molecules on metal surfaces, the use of adsorption models has been very common [44]. For this purpose the experimental data are seen in table 1 were adjusted by three different adsorption isotherm models such as Langmuir, Frumkin, Temkin and Freundlich. From all the employed isotherms, the best fitting and description of the adsorption behavior of the *P. persica* extract on the studied steel surface was obtained with Frumkin adsorption isotherm, which is represented by equation 5:

$$\text{Log } \frac{\theta C_{inh}}{1-\theta} = \text{log } K + g\theta \tag{5}$$

where K represents the adsorption at desorption equilibrium constant, C_{inh} is the concentration of inhibitor (GCI [ppm]) and g corresponds to the adsorbate interaction parameter. The covered surface degree (θ) was calculated by using the IE_w data reported in table 1 and equation (6):

$$\theta = \frac{IE_w}{100} \tag{6}$$

Table 1. CIE of *P. persica* extract on AISI 1018 Carbon steel in 0.5 M H₂SO₄ at 25 °C by weight loss

Temperature (°C)	GCI [ppm]	V _{corr} [mpy]	θ	IE _w [%]
25	0	219.18		-
	200	148.31	0.33	33
	300	145.21	0.34	34
	400	135.16	0.38	38
	500	92.24	0.38	58
	600	44.38	0.80	80
40	0	238.81		-
	200	173.37	0.2	20
	300	145.08	0.32	32
	400	131.67	0.37	37
	500	130.20	0.38	38
	600	129.12	0.38	38
60	0	260		-
	200	174.18	0.18	18
	300	162.11	0.22	22
	400	166.80	0.21	21
	500	139.45	0.31	31
	600	131.94	0.34	34

The figure 3 shows the dependence of the log (θCinh/1-θ) vs. θ, where a good fitting process can be observed, which was obtained with correlation coefficient (R²) data and the slope that are reported in table 2. The slope value indicates that the adsorption of the *P. persica* extract occurred on the metal surface [44]. In addition, the K values indicate a synergistic effect by the organic molecules present in the *P. persica* extract, which tend through a high electronic density zone located at the functional groups or aromatic rings to a fast orientation toward the steel surface.

Table 2. Standard free energy of adsorption data of the *P. persica* extract on AISI 1018 Carbon steel in 0.5 M H₂SO₄

Temperature	Slope	R ²	K _{ads}	-ΔG _{ads} ⁰ [kJ mol ⁻¹]
25	2.59	0.94	0.391	-22.45
40	4.452	0.96	0.224	-14.37
60	10.317	0.94	0.096	-9.54

In order to confirm the interaction between the CI and the steel surface, the standard free adsorption energy (ΔG_{ads}⁰) was calculated using Equation (7):

$$\Delta G_{ads}^0 = -2.303RT \log(55.5 K) \tag{7}$$

where R is the gas constant, 55.5 is the molar concentration of water in the solution and T is the absolute temperature. The ΔG_{ads}^0 values are reported in table 2 and fall within the interval $-9.54 \text{ kJmol}^{-1} \geq \Delta G_{ads}^0 \leq -22.45 \text{ kJmol}^{-1}$ at the evaluated temperatures.

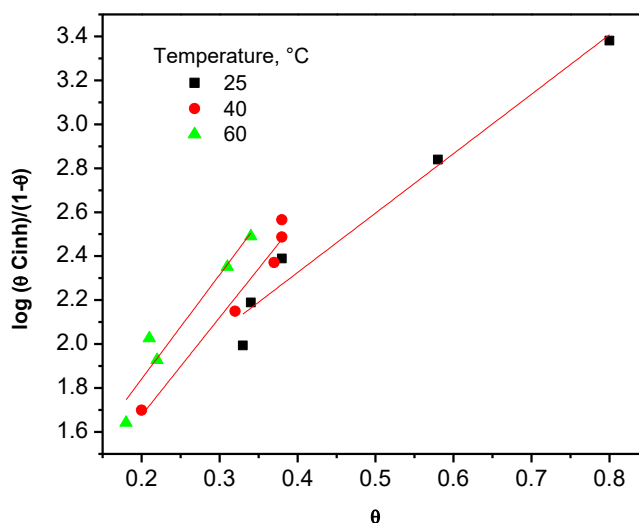


Figure 3. Frumkin adsorption isotherms from AISI 1018 Carbon steel in 0.5M H_2SO_4 with *P. persica* as GCI

The obtained negative values of ΔG_{ads}^0 indicate that the adsorption process of the *P. persica* extract on the steel surface is spontaneous. Alinnor and Ejikeme [45] and Umoren [46] obtained the related observations by evaluating plant extracts as GCIs. Most studies on GCIs have accepted the ΔG_{ads}^0 value interval to indicate when an adsorption process is physical or chemical. Small ΔG_{ads}^0 values (around -20.0 KJmol^{-1} or less negative) indicate a physical adsorption process, where the attraction and repulsion forces between the GCI and the metal surface prevail. On the other hand, ΔG_{ads}^0 values around -40 KJmol^{-1} or higher indicate a chemical adsorption process due to the formation of coordination bonds between the inhibitor and the steel surface. According to the aforesaid, the ΔG_{ads}^0 values (table 2) indicate that the adsorption process of the *P. persica* extract molecules is physical. According to Sharma [47] and Al-Haj-Ali [48] the decrease in CIE with temperature rise leads generally to a physical adsorption mechanism, because the weak interactions are broken by raising the temperature (desorption). According to the GC-MS analysis, the *P. persica* extract is rich in phytochemicals such as fatty acids and terpenes (see table 6). However, the most abundant component is α -Tocopherol (23.70 %) whose chemical structure features an aromatic ring and oxygen heteroatoms, being the zones with higher electronic density the ones that exert an effect on the electrostatic interactions with the surface of the energized metal, originating stable interactions [49].

Notwithstanding, it is clear that the purpose of the adsorption of phytochemical components is to protect the metal surface from the attack of the aggressive ions in the acid medium, but owing to the

complex chemical composition of the *P. persica* extract, it would be difficult to assign the inhibition effect to a particular phytochemical compound [50, 51].

3.2. Potentiodynamic polarization curves (PPCs)

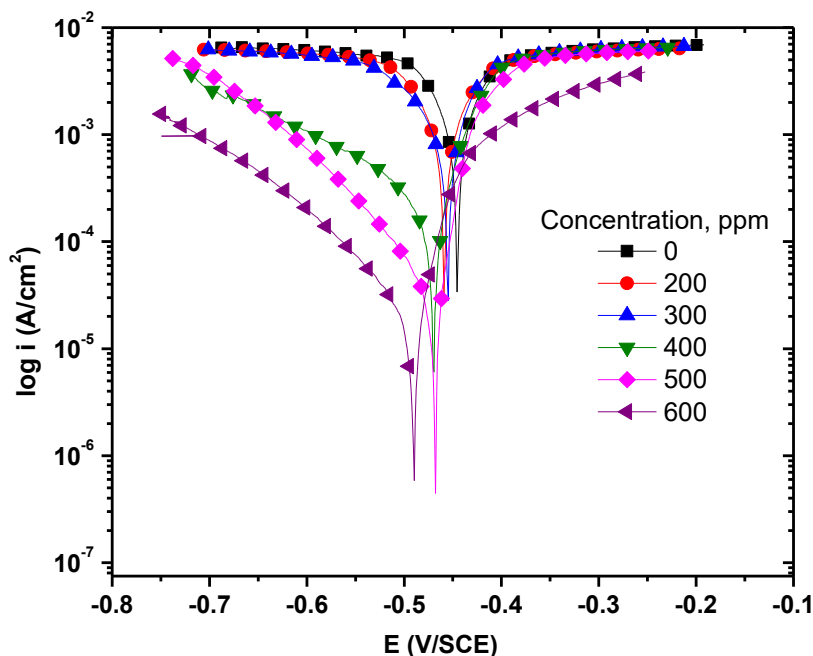


Figure 4. PPC at different concentrations of *P. persica* using AISI 1018 Carbon steel in 0.5 M H₂SO₄ at 25 °C

The figure 4 shows the PPCs of AISI 1018 Carbon steel in the absence and presence of *P. persica* extract in 0.5 M H₂SO₄ at 25 °C. It is observed that the presence of *P. persica* in the acid solution causes the displacement of the PPCs toward current density values that are lower than those displayed by the systems without GCI, which indicates that its addition reduces the steel corrosion rate in acid medium. This phenomenon is attributed to the presence of *P. persica* on the steel surface, which diminishes the kinetics of the anodic and cathodic reactions. At concentrations from 400 to 600 ppm, the diminution of i_{corr} is more evident because a higher amount of *P. persica* extract molecules in the corrosive medium compete for blocking the active sites from the presence of aggressive ions (SO_4^-) and water molecules. However, some active sites cannot be protected due to the presence of inclusions, grain boundary defects and the very topography of the steel surface, which as a whole, can generate the formation of microcells. The table 3 shows electrochemical parameters such as current density (i_{corr}) and anodic (β_a) and cathodic (β_c) slopes, which were obtained by Tafel extrapolation at the corrosion potential (E_{corr}), and IE_T as well.

Table 3 Electrochemical polarization parameters for AISI 1018 Carbon steel in 1.0 M H₂SO₄ as functions of the *P. persica* concentration at 25 °C.

GCI (ppm)	β_a (mV/dec)	$-\beta_c$ (mV/dec)	i_{corr} ($\mu\text{A}/\text{cm}^2$)	$-E_{corr}$ mV/SCE	$IE_T\%$
0	87	74	1010	445	-
200	316	78	810	458	20
300	341	78	600	482	41
400	298	62	377	466	63
500	207	39	955	475	91
600	232	69	82	493	92

The IE_T increase confirms that the *P. persica* extract affects the redox processes by blocking the active sites, indicating that the $(1-\theta)$ ratio decreases as the *P. persica* concentration increases. The analysis of the E_{corr} displacement in *P. persica* presence with respect to the blank, confirmed its displacement to more negative values within the interval ranging from 13 to 48 mV at the evaluated concentrations; then, the *P. persica* extract can be classified as a mixed-type inhibitor being preferably adsorbed on the cathodic zones of the evaluated steel [52]. Therefore, its presence in the metal-solution interface reduces the metal dissolution, but mainly the rate of the hydrogen evolution reactions. [53,54] Likewise, the β_c and β_a values did not feature any trend with the increasing *P. persica* concentration, which indicates that the inhibition process occurred through a blocking mechanism as a function of θ . [55, 56].

The figure 5 shows the behavior of the PPCs as a function of time at 600 ppm of *P. persica* extract used to inhibit the corrosion of AISI 1018 Carbon steel in 0.5 M H₂SO₄. It is observed that the current density at the cathodic and anodic branches tends to diminish with time; then, the electrostatic interactions between the inhibitor and the metal surface is controlled by the *P. persica* adsorption rate. This fact is confirmed in table 4, where it is observed that the maximum IE_T (97%) was obtained after 4 h whereas between 6 and 8 h, IE_T presents a gradual diminution associated with the degradation of the *P. persica* film formed on the steel surface, which originated low solubility iron corrosion products (melanterite, rosenite, szomolnokite, etc.) and oxyhydroxides (goethite), which together prevent the formation of a passive surface film. [57] Depending on the time, the *P. persica* extract presents properties of a mixed-type inhibitor with a preference toward the anodic branch. This fact indicates that the potential on the surface of the electrode will define the characteristics of the inhibitor and its adsorption mechanism.

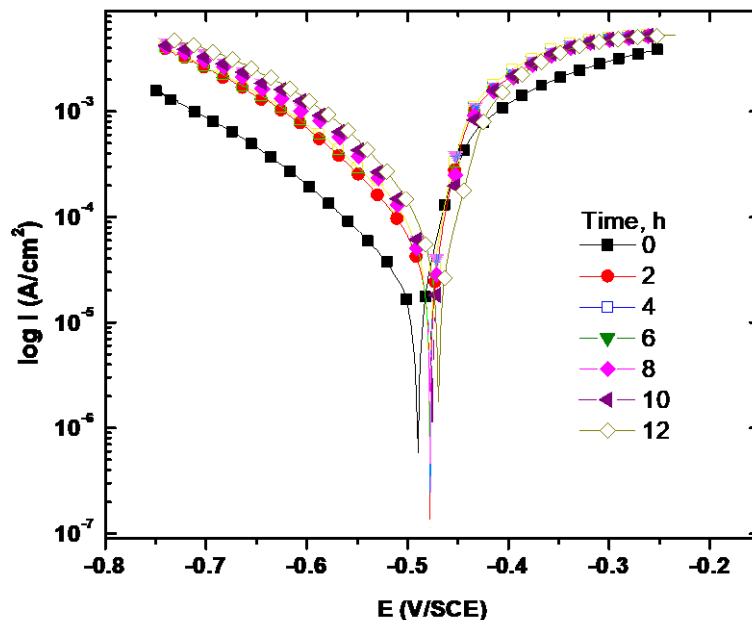


Figure 5. PPCs of residence time with 600 ppm of *P. persica* as GCI on AISI 1018 Carbon steel in 0.5 M H₂SO₄ at 25 °C.

Table 4. Electrochemical polarization parameters for AISI 1018 Carbon steel in 1.0 M H₂SO₄ as functions of time at 600 ppm of *P. persica* and 25 °C.

Time (h)	β_a (mV/dec)	$-\beta_c$ (mV/dec)	i_{corr} ($\mu A/cm^2$)	$-E_{corr}$ (mV/SCE)	$IE_T\%$
0	232	69	82	489	92
2	21	43	31	477	95
4	20	31	27	470	97
6	22	47	37	470	93
8	24	49	34	476	93
10	33	69	50	473	90
12	49.91	43.5	60	470	88

3.3. Electrochemical impedance spectroscopy (EIS)

In the figure 6 shows Nyquist diagrams as functions of the *P. persica* concentration as GCI of AISI 1018 Carbon steel in 0.5 M H₂SO₄ at 25 °C. The Nyquist diagrams show semicircles that are capacitive-like at high and intermediate frequency values and not perfect inductive semicircles at lower frequencies, which could be attributed to the relaxing process obtained due to the adsorption and desorption of species such as hydroxides and oxides on the electrode surface [58] without and with *P. persica* as green inhibitor. The depressed semicircles could be attributed to the frequency dispersion

effect, where at low frequency values, some elongations are observed, which are due to the accumulation of all kinds of species at the metal-solution interface [59]. The equivalent electrical circuits (EECs) used to adjust the steel impedance spectra in absence and presence of the *P. persica* extract are shown in figure 7, which consist of the solution resistance (R_s) and charge resistance (R_{ct}) associated with a constant phase element (C_{PE}) to substitute the condenser of double pure layer to model the deviation for an ideal capacitor; (R_L) is the resistance of ions migrating to the solution, which show a permanent and dominant inductance between a frequency range when n is the face displacement, which is associated with a non-ideal distribution of current as a result of the roughness and possible little defects on the metal surface [59].

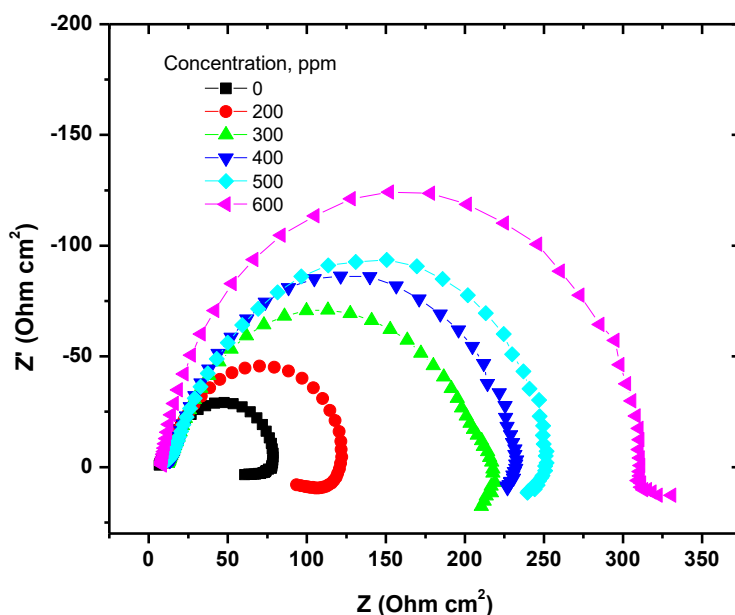


Figure 6. Nyquist diagrams of *P. persica* as GCI (0 -600 ppm) of AISI 1018 Carbon steel in 0.5 M H_2SO_4 at 25 °C



Figure 7. Equivalent circuits used for fitting data obtained by EIS from AISI 1018 Carbon steel in 0.5 M H_2SO_4 at 25 °C. (a) Without and with 200 ppm of green inhibitor; (b) with 300 to 600 ppm of *P. persica* used as GCI.

From table 5, it is observed that R_{ct} increases significantly with the concentration of the *P. persica* extract as GCI. The analysis of the R_{ct} values indicates a direct relationship with the adsorption of the molecules present in the *P. persica* extract, where the nucleophilic and hydrophobic parts of the molecules occupy active sites to reject the corrosive medium. From the analysis of C_{dl} , it is clear that it

diminishes with the increase in the *P. persica* concentration, which indicates that the dielectric defects in the interface are reduced, because the dielectric constants of the water molecules are higher than those displayed by the *P. persica* extract. This fact promoted the occurrence of a phenomenon implying the displacement of water molecules by the *P. persica* extract on the steel surface, indicating that at low C_{dl} values, the desorption of water molecules is faster according to the *P. persica* concentration. In order to better understand the surface phenomena, the use of C_{PE} and n was considered, which are related to different physical phenomena, for example, surface heterogeneity, which results from surface roughness, impurities, dislocations, distribution of the active sites, adsorption of inhibitors and formation of porous layers [60].

Table 5. EIS data from AISI 1018 Carbon steel in 0.5 M H₂SO₄ at 25 °C with *P. persica* as GCI

GCI (ppm)	$R_s/\Omega\text{ cm}^2$	$R_{ct}/\Omega\text{ cm}^2$	$C_{dl}/\mu\text{F cm}^{-2}$	$C_{PE}/\mu\text{F cm}^{-2}$	n	$IE_{EIS}\%$
0	4.3	57	90.0	120	0.90	-
200	9.2	70	72.0	103	0.89	19
300	13.2	202	39.3	98	0.88	72
400	13.0	222	35.8	96	0.87	74
500	12.0	241	34.0	95	0.88	76
600	8.4	304	26.1	47	0.87	81

The diminution of the C_{PE} values as a function of the *P. persica* concentration can be correlated with an increase in θ by effect of the *P. persica* adsorption on the steel surface whereas the n values have a direct relationship with the surface characteristics to be protected [59]; in this case, they are slightly lower with inhibitor, indicating that the adsorption of the *P. persica* molecules, because of their high molecular weights and asymmetric molecular configurations with respect to the corrosion products, generate a more irregular metal-solution interface. The inhibition efficiency (IE_{EIS}) by EIS was calculated by means of Equation 7:

$$IE_{EIS}, \% = \frac{R_{ct2} - R_{ct1}}{R_{ct2}} \tag{7}$$

where R_{ct1} and R_{ct2} are the transfer resistance values with and without GCI. Likewise, the IE_{EIS} values reported in table 5 present a relationship that is directly proportional to the *P. persica* concentration increase. This very behavior was also observed with the previous techniques, where IE_W and IE_T were calculated whereas the double layer capacitance values were calculated by employing the next equation:

$$C_{dl} = \frac{1}{2\pi f_{max} R_{ct}} \tag{8}$$

where f_{max} corresponds to the frequency with the maximum value of imaginary impedance: $-Z_{im}(\text{max})$.

Double layer capacitance values were obtained according to equation 8, where the maximum value of imaginary impedance is found (f_{max}). In order to know the stability of the *P. persica* inhibitor as a time function, it was evaluated for 12 h. The figure 8 shows the EIS spectra, where an increase in the semicircle diameters with respect to time due to the *P. persica* adsorption can be observed, reaching a maximum residence time of 6 h, which is a time where the protective layer of *P. persica* molecules is at its maximum point and stable on the steel surface [61, 62].

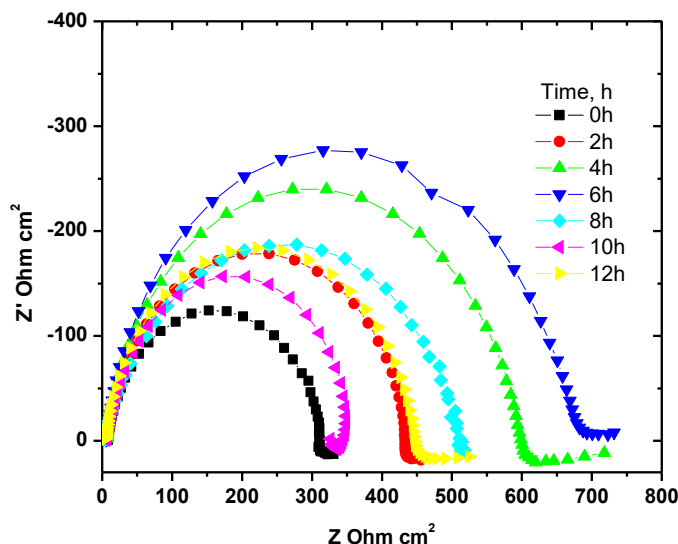


Figure 8. EIS for residence time of *P. persica* at 600 ppm on AISI 1018 Carbon steel in 0.5 M H₂SO₄ at 25 °C

3.4. Green corrosion inhibition mechanism

In agreement with Dariva & Galio and considering that the natural extracts studied as CIs are complex mixtures of different kinds of organic compounds, it is possible to state that the chemical molecular diversity is a good characteristic of GCIs, which frequently, in most cases, can be protonated or deprotonated, and the new formed species affect the active sites, both anodic and cathodic, on the steel surface, forming a simultaneous interaction with anodic and cathodic sites on the metal surface [63]. This fact explains why in different studies on GCIs, it has been stated that they act as mixed-type GCIs.

On the other hand, derived from what was said above, two hypothetical situations can be used to explain the inhibition mechanisms; in this sense, it is necessary to consider that during the first adsorption step of organic inhibitor on the metal surface, the substitution of water molecules by CI molecules adsorbed on the metal surface generally occurs as follow equation 9 [64]:



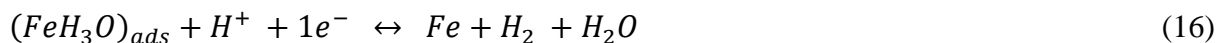
Likewise, the inhibitor could be combined with new Fe^{2+} ions formed on the metal surface, producing metal-inhibitor complexes as shown by equation 10 and 11:



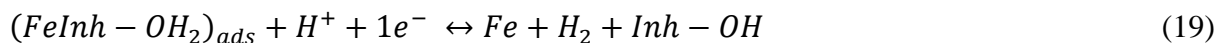
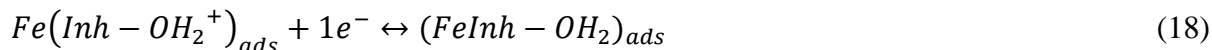
Commonly, the GCIs contain different compounds and they include atoms such as oxygen and nitrogen in their chemical structures. However, the oxygen atom is interesting because it has electronic wealth and it can act on the metal surface, but it can also be protonated in acid environment when it is present as a primary or secondary alcohol in organic natural compounds (equation 12). Likewise, the oxygen of fatty acids, in presence of an acid, tends to ionize anionic species (deprotonate, equation 13). For each case, it is possible to consider the interaction with ions in an acid environment in the corrosion inhibition mechanisms, which can be represented by the following general reactions:



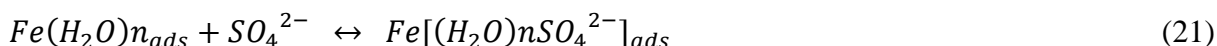
The cathodic reactions, in the absence of GCI can be summarized as follows [37]:

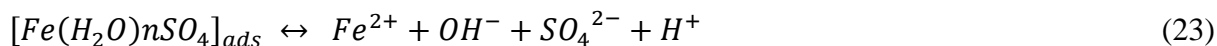
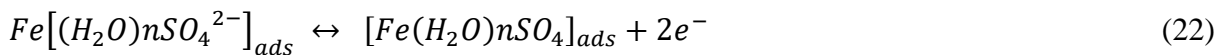


Whereas in the presence of GCI:

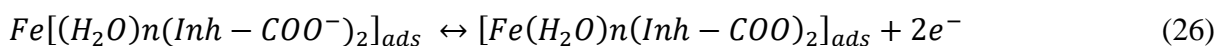
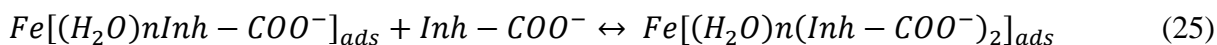


The adsorption of water molecules facilitates the adsorption of anions such as SO_4^{2-} on the metal surface when the reaction is without inhibitor, but the presence of GCI could promote the presence of a negative charge after deprotonation ($Inh-COO^{-}$) and form a “protective multilayer” on the corrosion products, restraining their dissolution and consequently, preventing the iron dissolution from continuing. These reaction routes are in agreement with the corrosion products and the anodic reactions in the absence of CI [37], which can be summarized as follows:





Whereas in the presence of GCI, the mechanism reactions can be described as follows:



In this way, the natural inhibitor forms adsorbent multilayers and they are stabilized by London dispersion forces formed between the long chains (hydrophobic portion) of the fatty acids and their esters [65, 66]. Through these multilayers, the active sites on the metal surface are blocked and as consequence, the corrosion rate is reduced.

Depending on the relative solubility of the newly formed complex, it can inhibit or catalyze the metal dissolution, increasing the metal corrosion rate [67]. A low *P. persica* concentration (200 ppm) cannot form compact complexes with the metal ions and a few formed complexes are soluble in the electrolyte solution, however, in high concentrations (600 ppm) of *P. persica* extract, double layer compact complexes are formed, protecting the metal surface and increasing the GCI efficiency to 94 % at 6 h of resident time.

3.5. Scanning Electronic Microscopy and Energy Dispersive X-Ray Spectroscopy (SEM and EDX micrographs)

The figure 9 shows the steel surface micrographs in absence and presence of *P. persica* extract immersed in 0.5 M H₂SO₄ for 6 h. In the figure 9(a), severe damage caused by the direct interaction between the corrosive medium and the steel surface can be observed. A film of corrosion products can be identified on the steel surface displaying both clear porosity and cracks. The presence of corrosion products on the metal surface is supported by the EDX analysis of figure 9(b), where intense signals of sulfur and oxygen can be seen, which are the result of the presence of per hydroxides, sulfates and sulfur compounds that are formed through the combination of oxygen and the sulfate ion present in the corrosive medium. The figure 9(c) shows the steel surface when it is protected with 600 ppm of *P. persica* extract and it can be clearly observed that the steel surface topography is more uniform, which indicates that most active sites were blocked by the *P. persica* extract protective action as inhibitor of the redox processes. Due to the aforementioned, the Fe and Mn signals in figure 9(d) are more intense in the analyzed area because they represent matrix elements without corrosion products or with a slight presence.

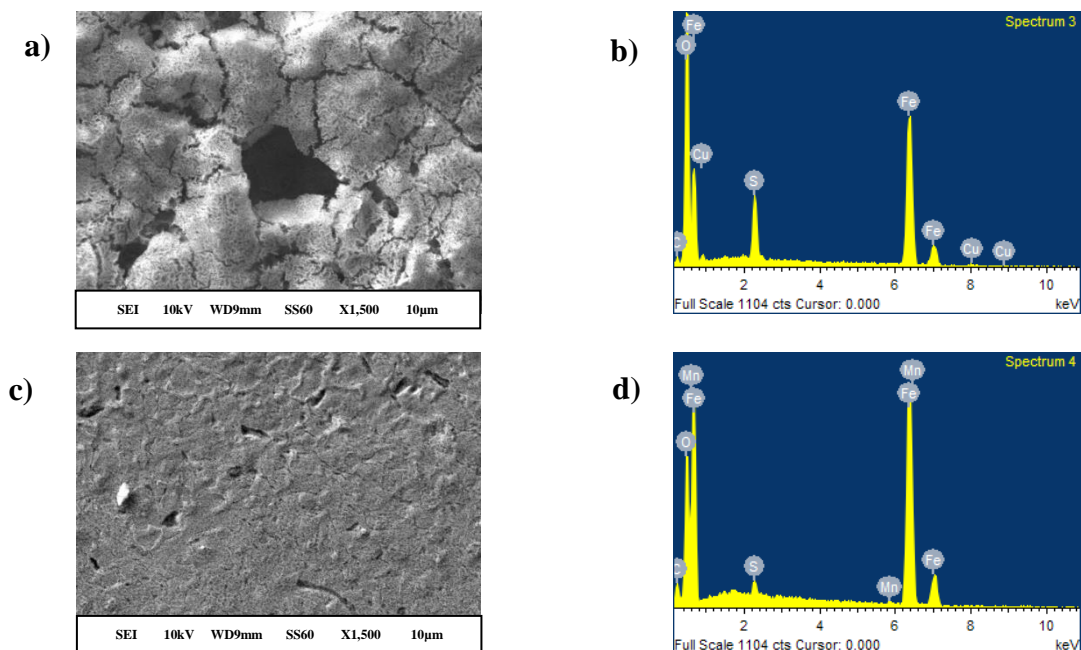


Figure 9. SEM and EDX micrographs from AISI 1018 Carbon steel in 0.5 M H_2SO_4 at 25 °C for 6 h, without GCI (a, b) and with 600 ppm *P. persica* (c, d).

3.6. Infrared spectroscopy inhibitor characterization

Some authors have stated and agreed with the fact that corrosion inhibition takes place and occurs as a result of the interaction between the metal and the extract. The infrared spectroscopy characterization of the extract from *P. persica* leaves was performed to identify the functional groups present in it. The infrared spectrum of crude extract is presented in figure 10, which reveals the main frequency regions and characteristic signals of functional groups from the different compounds present in the *P. persica* extract. The principal vibrational bands corresponded to the 2933 cm^{-1} signal assigned to the C-H bond in $-\text{CH}_3$ and $-\text{CH}_2$ present in alkanes; at 1608 cm^{-1} , the signal of carbon-to-carbon double bonds ($-\text{C}=\text{C}-$) from unsaturated compounds was observed; at 1365 cm^{-1} , the signal was assigned to the $-\text{CH}_2-$ methylene bond, and finally, the oxygen signal corresponding to the hydrogen bond (O-H) from a primary alcohol could be distinguished at 1076 cm^{-1} . The presence of oxygen and nitrogen atoms in the extracts met the general characteristics of typical GCIs as well [68].

3.7. GC-MS analysis of the GCI

Fractions of crude natural extracts whose composition can vary widely, since the GCIs are a homogeneous mixture of organic natural compounds were analyzed. The chemical content in the *P. persica* extract, relative percentages of each NP (afterwards separated by GC), retention times and ion mass [m/z] were established for each compound and the characteristic fragmentation pattern is summarized in table 6.

A total of ten compounds were identified, and the sum of the relative abundances for all of them represented 99.37 % of the total area; only one compound was not identified with the equipment

mass library. The chemical structures of the identified compounds are shown in figure 10, where most of them are terpenes [69].

Table 6. Natural organic compounds contended in the *P. persica* extract by MS

Systematic name of chemical compound (Synonym , % of relative abundance, identification number*)	t _r ^{&} (min)	[M ⁺]	Fragmentation by MS
(1R,5R)-2,6,6-Trimethylbicyclo[3.1.1]hept-2-ene (α-Pinene , 2.64 %, X)	6.16	136	121, 105, 93, 77, 63, 41
(1S,5S)-6,6-dimethyl-2-methylenbicyclo[3.1.1]heptane ((-)-β-Pinene , 16.05 %, XI)	6.89	136	121, 107, 93, 79, 69, 53, 41
7-Methyl-3-methylene-1,6-octadiene (β-Myrcene , 4.67 %, XII)	7.01	136	121, 107, 93, 79, 69, 53, 41, 27, 15
1-methyl-3-(1-methylethyl)-benzene (β-Cymene , 3.30 %, XIII)	7.67	134	119, 91, 77, 65, 39
1-methyl-4-(1-methylethyl)-1,4-cyclohexadiene (γ-Terpinene , 11.19 %, XIV)	8.21	136	121, 93, 77, 51, 43, 27
9,12,15-octadecatrienoic, methyl ester (Linoleic acid , 1.87 %, XV)	20.81	292	236, 191, 173, 149, 135, 121, 108, 79, 67, 55, 41
NID. (17.36 %, XVI)	20.92	429	----
2,6,10,15,19,23-Hexamethyltetracosane (2,6,10,14,18,22-hexaene) (Squalene , 7.47 %, XVII)	29.92	410	367, 341, 328, 299, 273, 231, 217, 175, 149, 137, 121, 95, 81, 69, 41
(2R)-2,5,7,8-Tetramethyl-2-[(4R,8R)-4,8,12-trimethyltridecyl]-6-chromanol (α-Tocopherol , 23.70 %, XVIII)	34.01	430	414, 388, 358, 316, 288, 274, 219, 165, 149, 121, 91, 43
17-(5-Ethyl-6-methylheptan-2-yl)-10,13-dimethyl-2,3,4,7,8,9,11,12,14,15,16,17-dodecahydro-1H-cyclopenta[β]phenanthren-3-ol (β-Sitosterol , 11.79 %, XIX)	37.56	414	396, 381, 354, 329, 303, 273, 255, 231, 213, 199, 173, 145, 133, 119, 81, 69, 43, 29

*Chemical structure, [&] GC retention time; [M⁺] molecular mass ion; NID = Not identified

The identified of natural compounds are mentioned in this order: from the highest to the lowest relative abundance; there is α -Tocopherol (23.70 %; **XVIII**); (-)- β -Pinene (16.05 %; **XI**); β -Sitosterol (11.79 %; **XIX**) and γ -Terpinene (11.19 %; **XIV**), Squalene (7.47 %, **XVII**); (-)- β -Myrcene (4.68 %, **XII**), β -Cymene (3.31 %, **XIII**), α -Pinene (2.64 %, **X**) and Linoleic acid (1.79 %, **XV**).

The most abundant NP in the *P. persica* extract was α -Tocopherol (23.70 %) and it is best known as vitamin E. It was previously identified in some vegetable species that showed antioxidant activity and vitamin E displayed stability at different temperatures [70, 71]. Recently, it was reported that the Cu and Cu40Zn surfaces immersed in stearic acid were protected by vitamin E with 99 % of corrosion IE, because of the improvement of the as-prepared hydrophobic layer against corrosion [66].

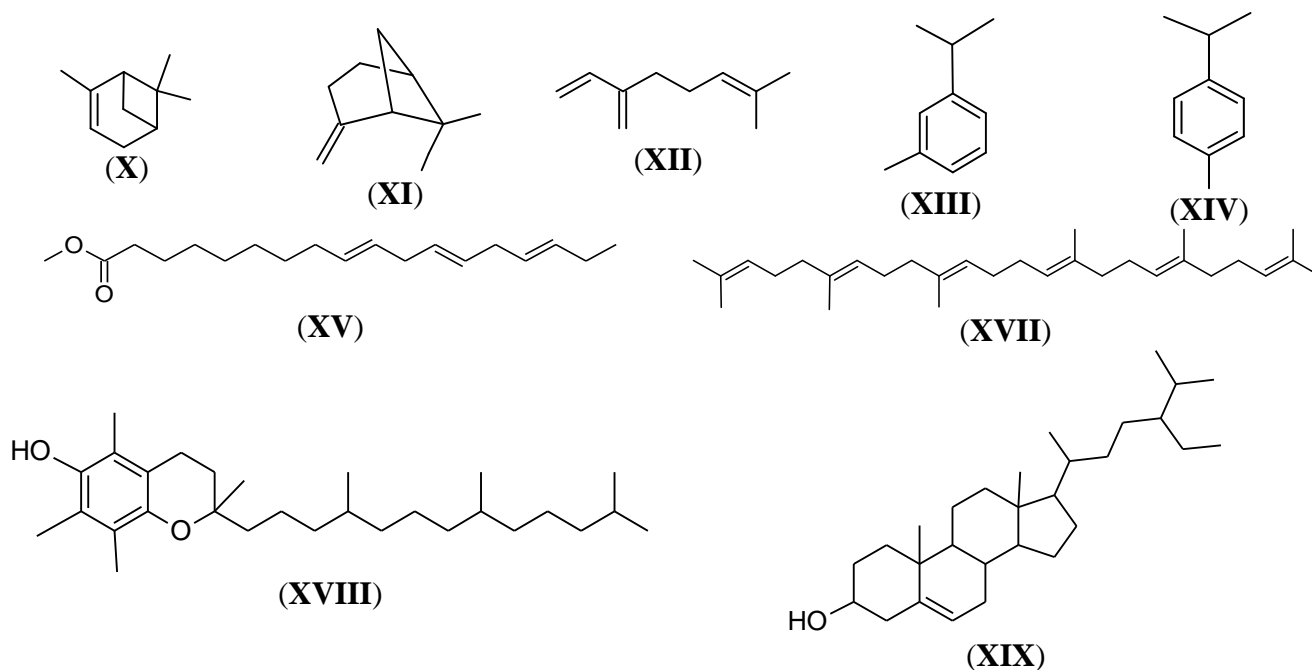


Figure 10. Natural compounds identified in the *P. persica* extract by GC-MS

Terpenes such as sterols were previously found through GC-MS in the extract from *Cynara scolymus* flowers, and in the ethanol extract from *Ficus hispida* leaves. Both extracts were studied as GCIs, and from the weight loss results, it was found that 1000 ppm of extract from *C. scolymus* flowers produced 89.0 % of corrosion IE on 1018 carbon steel in 0.5 M H₂SO₄ [70]; and 90.0 % of CIE was achieved by using 250 ppm of *F. hispida* ethanol extract against corrosion of mild steel in 1.0 M HCl through impedance [71]. Recently, β -Sitosterol was isolated from *Oryza sativa* L. (rice), and it was studied as GCI of mild steel in 1.0 M H₂SO₄, reaching 95.0 % of CIE, which was obtained by the weight loss technique at 30 °C [73].

Some authors reported the adequate CIA of essential oils and found monoterpenes such as *Citrus aurantium* in the chemical content of essential oil from fresh peels by GC-MS, which protected steel in 1 M HCl, reaching a CIE of 95.0 % when using 5 g/L of inhibitor [74]. The same experience occurred with *Chenopodium ambrosioides*, which protected carbon steel in H₂SO₄, reaching a CIE of 94.0 % by using 4 g/L of GCI [75] whereas some specific monoterpenes identified for *P. persica* in this work were found and studied in other works, for example, in the essential oil of *Thymus algeriensis*, these compounds were found as part of the chemical content: α - and β -Pinene, Myrcene and Cymene. The essential oil from *T. algeriensis* protected mild steel in 1.0 M HCl and reached 81.0 % of CIE after using 1.0 g/L of GCI [75].

The chemical analysis of pistachio (*Pistacia vera*), essential oil of the unripe fruits, showed a high content of α -Pinene (54.2 %) and β -Pinene not exceeding 1 %. The pistachio essential oil was studied as a GCI on carbon steel in 0.5 M H₂SO₄ and reached 81.64 % of CIE after using 1.0 g/L [76]. The CIA of essential oil from *Carum carvi* was studied with mild steel in H₂SO₄ reaching 86.0 % after using 50 ppm. The chemical composition determined by GC-MS showed the presence of β -Pinene and β -Myrcene and other compounds in the extract [77]. In the cinnamon (*Cinammomum verum*) essential

oil, chemical compounds such as γ -Terpinene were identified in low abundance by GC-MS; this compound was studied as GCI from the cinnamon essential oil on copper in 0.5 M H_2SO_4 , reaching 79.31 % after employing 300 ppm [78].

The diversity in members and kinds of compounds present in the extracts, wherever the species comes from, complicates the decision of assigning the compounds responsible for the activity as GCI. After observing and analyzing the chemical results obtained in this work for *P. persica*, it is possible to consider by their present in a high abundance in the GCI that α -Tocopherol and β -Sitosterol are the phytochemicals which could be attributed the CIA against AISI 1018 Carbon steel in H_2SO_4 .

The GCI could be used in chemical pickling of steel, where sulfuric acid is employed or in chemical pickling of ferrous metals because the oxide is partially eliminated before the total pickling from the surface. And also in corrosion inhibition with acid environments that use short exposure times. Due to the fact that the natural inhibitor is completely soluble in sulfuric acid and the residence time is almost 6 h, at 25 °C, the natural chemical compound of *P. persica* results interesting because it contains hydrocarbon chains and nitrogen or oxygen in compounds such as α -Tocopherol in its chemical structure and it has been reported that it is stable at different temperatures to protect copper [51, 80].

3.8. Toxicity bioassays

Natural and synthetic chemicals, food supplies, health care, industries and safe sanitation are essential to our daily lives. At the same time, the protection of all ecosystems through responsible practices is paramount. Since the 1970s, the monitoring of persistent, bioaccumulative and toxic chemicals used by analytical chemistry has provided important spatial and temporal data trends in important contexts from human health to pollution and biodiversity protection.

Plants produce known and unknown phytochemicals, and they are considered as “natural or organic compounds” and therefore safer especially because inherited knowledge of ancient communities that used medicinal plants in their traditional medicine, however, there is scarce scientific evidence to support this belief [81]. Recent scientific evidence has revealed that many plants considered to be medicinal are potentially toxic, mutagenic and carcinogenic [82]. It is suitable and scientifically correct to study GCIs; it does not matter if they come or not from medicinal plants because it is necessary to confirm the possibility that the used concentrations are really harmless for humans and the environment.

The interest in studying the GCI that comes from the *P. persica* leaves through the *A. salina* lethality is aimed at discarding any toxicity possibility and confirming that it could be used safely because it does not provoke negative consequences. It is important to indicate that this is the first time a biological evaluation is included as a toxicological study of a GCI. In this work, we used two cheap and easy bioassays; they were the lethality of brine shrimp (*A. salina*) and toxicity against Lettuce (*L. sativa*) seeds, which play a significant role in toxicity tests from isolated chemicals, pesticides, and environmental samples. Both assays give information to close up some possible environmental applications of green inhibitors. The goal in this work was to explore and know closely the environmental impact of *P. persica* and if it can be used as a GCI.

3.8.1. Lethality of *Artemia salina* Leanch (*A. salina*)

The lethal medium concentration (CL_{50}) and the confidence intervals at 95 % were calculated by Probit analysis [41] from extract *P. persica* leaves and crossed with the established category for environmental toxic substances proposed by Fernández et al., 2006 [83]. The results showed that the extract of *P. persica* leaves CL_{50} had 1568 ppm, and indicated that this is the necessary concentration of inhibitor to produce 50 % of dead to *A. salina*, however, the active concentration as GCI was 600 ppm, which is lower than that of LC_{50} ; in the first instance it can be mentioned that the 600 ppm of extract of *P. persica* leaves almost reached 80 % (weight loss) of corrosion IE and are not toxic for *A. salina*.

3.8.2. *Lactuca sativa* germination bioassay

The germination index (GI) from *L. sativa* was calculated with equation 20. And the development inhibition of both radicle and hypocotyl from *L. sativa* was calculated with equation 21.

$$IG\% = \frac{RGS * RDR}{100} \quad (20)$$

where *RGS* is the relative germination of seeds and *RDR* is the relative radicle development.

$$\% \eta = \frac{\bar{x}_t - \bar{x}_e}{\bar{x}_t} * 100 \quad (21)$$

where $\% \eta$ is the inhibition percentage of either the radicle or hypocotyl, \bar{x}_t is the average length for the negative control (without extract) and \bar{x}_e is the average length for the treatment (with extract).

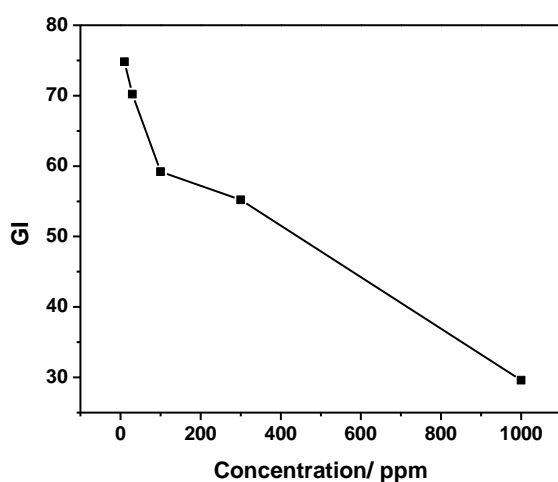


Figure 11. Germination index of *L. sativa* seeds in the presence of extract of *P. persica* leaves

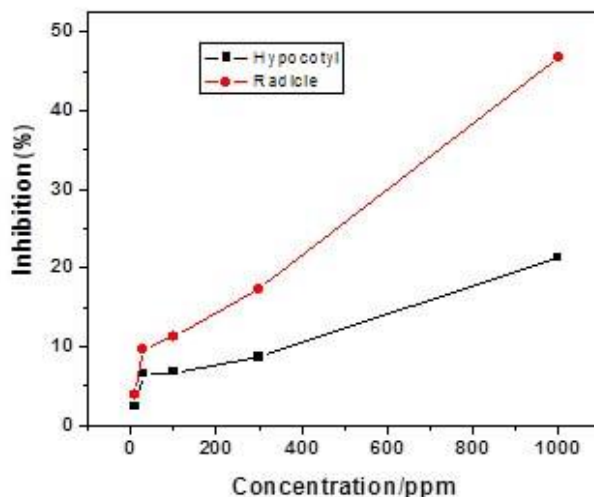


Figure 12. Development reduction percentages of hypocotyl and radicle of *L. sativa* by extract of *P. persica* leaves.

The figure 11 shows that the germination index decreased when the concentration of the *P. persica* extracts increased. The germination index of *L. sativa* was almost 30 % due to the influence of 600 ppm of *P. persica* extract. The figure 12 shows the inhibition of the developed (%) radicle and hypocotyl produced by the *P. persica* extract.

The inhibition percentage increased as the extract concentration increased. At 1000 ppm of *P. persica* extract caused a development reduction of 45 % for the radicle and of 13 % for hypocotyl. It is seen that lettuce seeds were highly sensible at the assayed concentrations of *P. persica* extract.

4. CONCLUSIONS

The present work showed that 600 ppm of *P. persica* extract are good for the corrosion inhibition of AISI 1018 Carbon steel in 0.5 M H₂SO₄ at 25 °C as this concentration reached a 80.0 % of CIE through weight loss. The PPC evidenced that the *P. persica* extract acts as a mixed-type inhibitor with cathodic predominance. The EIS confirmed that the residence time was 6 h and that the inhibitor was stable in the aggressive solution. The micrographs show that in the *P. persica* presence, the metal surface presents less damage due to the blockage of the steel active sites by the inhibitor. A high abundance of vitamin E (α -Tocopherol) and β -Bitosterol was detected by GC-MS in the phytochemicals; these compounds, which were part of the extract from *P. persica* leaves, were associated with the CIE.

The concentration of *P. persica* extract as a good GCI was nontoxic against *A. salina*, however at the same concentration turned to be lower toxic against *L. sativa*, because it affected the germination of seeds and radicle development. In order to ensure that the GCIs do not represent environmental and ecological risks, assessment was important and relevant to demonstrate that they are safe for humans

and the environment at the concentration that reached good corrosion IE, independently of the source they come from (synthetic, inorganic or organic and natural), which is the case of phytochemicals. Meanwhile, the extract of *P. persica* leaves is a good GCI and it could be classified as slightly toxic.

ACKNOWLEDGEMENTS

The authors are grateful to the BUAP-VIEP and the National Analytical Laboratory at the Center of Chemical Investigations of the Autonomous University of Morelos State, which provided the facilities and technical assistance to carry out some chemical analysis.

References

1. A. Döner, R. Solmaz, M. Özcan, and G. Kardaş, *Corros Sci*, 53 (2011) 2902.
2. M.A. Quraishi, J. Rawat, *Mater Chem Phys*, 73 (2011) 118.
3. Y. R Liu, Z. M. Gao, Z. Zhang and D. F. Shi, *Corrosion Sci Prot Technol*, 19 (2007) 323.
4. G. Gece, *Corros Sci*, 53(2011) 3873.
5. S. A. Kumar, A. Sankar, S. R. Kumar, and M. Vijayan, *AJRC*, 6 (2013) 3.
6. D. Guzmán-Lucero, O. Olivares-Xometl, R. Martínez-Palou, N. V. Likhanova, M. A. Domínguez-Aguilar, and V. Garibay-Febles, *Ind Eng Chem Res*, 50 (2011) 7129.
7. S.E. Manahan, *Environmental chemistry*, 6th ed., Lewis, Boca Raton, 1994.
8. S. Umoren, I. Obot and I. Igwe, *TOCORRJ*, 1(2008) 1.
9. J. M. Bastidas, P. Pinilla, E. Cano, J. L. Polo, and S. Miguel, *Corros Sci*, 45(2003) 427.
10. X. Pang, X. Ran, F. Kuang, J. Xie, and B. Hou, *Chin J Chem Eng* 18 (2010) 337.
11. F. B. Mansfeld, *Corrosion Mechanism*, Marcel Dekker (1987), New York. USA.
12. I. B. Obot, and N. O. Obi-Egbedi, *Curr App Phys*, 11(2011) 382.
13. P. Mourya, S. Banerjee, and M. M. Singh, *Corr Sci*, 85 (2014) 352.
14. C. Loganayagi, C. Kamal, and M. G. Sethuraman, *ACS Sustain Chem Eng*, 2 (2014) 606.
15. R. G. Suarez-Hernandez, J. F. Gonzalez-Rodriguez, G. Dominguez-Patiño, and A. Martinez-Villafañe, *Anti Corros Method M*, 61(2014) 224.
16. N. Odewunmi, S. Umoren, and Z. Gasem, *J Ind Eng Chem*, 21 (2015) 239.
17. G. Ji, S. Anjum, S. Sundaram, and R. Prakash, *Corros Sci*, 90 (2015) 107.
18. A. Ostovari, S. M. Hoseinie, M. Peikari, S. R. Shadizadeh, S. J. Hashemi, *Corros Sci*, 51 (2009) 1935.
19. M. Lebrini, F. Robert, A. Lecante, and C. Roos, *Corros Sci*, 53 (2011) 687.
20. M. Lebrini, F. Robert, P. A. Blandinieres, and C. Roos, *Int J Electrochem Sci*, 6 (2011) 2443.
21. O. K. Abiola, N. C. Oforka, E. E. Ebenso, and N. M. Nwinuka, *Anti Corros Method M*, 54 (2007) 219.
22. G. O. Avwiri, and F. O. Igho, *Mater Lett*, 57 (2003) 3705.
23. B. G. Clubley, *Chemicals Inhibitors for Corrosion Control*, Royal Society Chemistry, 1990, London.
24. P. Muthukrishnan, B. Jeyaprabha, and P. Prakash, *Int J Ind Chem*, 5 (2014) 1-11.
25. M. Tezeghdenti, L. Dhouibi, and N. Etteyeb, *J Bio Tribo Corros*, 1(2015) 1.
26. S. N. Nichenametla, T. G. Taruscio, D. L. Barney, and J. H. Exon, *Crit Rev Food Sci Nutr*, 46 (2006) 61.
27. B. A. Cevallos-Casals, D. Byrne, W. R. Okie, and L. Cisneros-Zevallos, *Food Chem*, 96 (2006) 273.
28. G. Noratto, W. Porter, D. H. Byrne, and L. Cisneros-Zevallos, *J Agric Food Chem*, 57 (2009) 5219.
29. P. R. Nilo, R. Campos-Vargas, and A. Orellana, *J Proteomics*, 75 (2012) 1618.

30. T. K. Lim, *Edible medicinal and non-medicinal plants: Fruits*, Springer, 2012, New Delhi, India.
31. F. A. Tomás-Barberán, M. I. Gil, P. Cremin, A. L. Waterhouse, B. Hess-Pierce, and A. A. Kader, *J Agric Food Chem*, 49 (2001) 4748.
32. S. Chandra, and M. S. Sastry, *Indian J Pharm Sci*, 50 (1998) 321.
33. C. Andreotti, D. Ravaglia, A. Ragaini, and G. Costa, *Ann Appl Biol*, 153 (2008) 11.
34. A. Z. D. Valle, I. Mignani, A. Pinardi, F. Galvano, and S. Ciappellano, *Eur Food Res Technol*, 225 (2007) 167.
35. A. Rodríguez-Torres, M. G. Valladares-Cisneros, and J. G. González-Rodríguez, *Int J Electrochem Sci*, 10 (2015) 4053.
36. M. Finšgara, and J. Jackson, *Corros Sci*, 86 (2014) 17.
37. N. V. Likhanova, M. A. Domínguez-Aguilar, O. Olivares-Xometl, N. Nava-Entzana, E. Arce, and H. Dorantes, *Corros Sci*, 52 (2010) 2088.
38. S. Omanovic, and S. G. Roscoe, *Langmuir*, 15 (1999) 8315.
39. B. M. Meyer, N. R. Ferringni, J. E. Putnam, L. B. Jacobsen, D. E. Nichols, and J. L. McLaughlin, *Planta Medica*, 45 (1982) 31.
40. Z. S. Ferraz Filha, J. A. Lombardi, L. S. Guzzo, and D. A. Saúde-Guimaraes, *Rev. Bras. Pl. Med, Botucatu*, 14 (2012) 358.
41. D. J. Finney, *Probit analysis*. New York: Cambridge University Press, 1971, USA.
42. F. M. Rodrigues da Silva Junior, E. M. Garcia, P. R. M. Baisch, N. Mirlean, and A. L. Muccillo-Baisch, *Soil Water Res*, 8 (2013) 56.
43. A. Hamdy, Sh. Nour, El-Gendy, *Egyptian Journal of Petroleum*, 22 (2013) 17.
44. F. O. Nwosu, L. A. Nnanna, O. Osarolube, *Int J Mater Chem*, 3 (2013) 64.
45. I. J. Alinnor, and P. M. Ejikeme, *Amer Chem Sci J*, 2 (2012) 122.
46. S. A. Umoren, I. B. Obot, E. E. Ebenso, and N. O. Obi-Egbedi, *Desalination*, 247 (2009) 561.
47. A. Sharma, G. Choudhary, A. Sharma, and S. Yadav, *IJIRSET*, 2 (2013) 7982.
48. A.M. Al-Haj-Ali, N. A. Jarrah, N. D. Muazu, R. O. Rihan, *J. Appl. Sci. Environ. Manage*, 18 (2014) 543.
49. S. K. Saha, A. Dutta, P. Ghosh, D. Sukul, and P. Banerjee, *Phys Chem Chem Phys*, 18 (2016) 17898.
50. P. Muthukrishnan, P. Prakash, M. Ilayaraja, B. Jeyaprabha, and K. Shankar, *Metall and Materi Trans B*, 46 (2015) 1448.
51. P. M. Ejikeme, S. G. Umana, and O. D. Onukwuli, *Port Electrochim Acta*, 30 (2012) 317.
52. C. Cao, *Corros. Sci.*, 38 (1996) 2073.
53. P. Muthukrishnan, B. Jeyaprabha, and P. Prakash, *Acta Metall Sin*, 26 (2013) 416.
54. A. Y. Musa, A. B. Mohamad, M. S. Takriff, and R. T. T. Jalgham, *Res Chem Intermed*, 38 (2012) 453.
55. S. A. Umoren, I. O. Obot, and Z. M Gasem, *Ionics*, 2015, 21: 1171-1186.
56. A. Bousskri, A. Anejjar, M. Messali, R. Salghi, O Benali, Y. Karzazi, S. Jodeh, M. Zougagh, EE. Ebenso, B. Hammouti. *J Mol Liq*. 211(2015) 1000.
57. O. Olivares-Xometl, N. V. Likhanova, N. Nava, A. Cabral Prieto, I. V. Lijanova, A. Escobedo-Morales, C. López-Aguilar, *Int. J. Electrochem. Sci.*, 8 (2013) 735
58. X. Li, S. Deng, and H. Fu, *Corros Sci*, 62 (2012) 163.
59. M. Özcan, I. Dehri, and M. Erbil, *Appl Surf Sci*, 236(2004) 155.
60. M.E. Orazem, B. Tribollet, *Electrochemical Impedance Spectroscopy*, 2008, John Wiley & Sons, Inc., New Jersey.
61. R. Solmaz, G. Kardas, M. Culha, B. Yazici, and M. Erbil, *Electrochim Acta*, 53 (2008) 5941.
62. A. K. Singh, and M. A. Quraishi, *Corros Sci*, 51 (2010) 152.
63. C. G. Dariva and A. F. Galio, *Developments in corrosion protection*, 16 (2014) 365.
64. M. M. Saleh, *Mater. Chem. Phys.* 98 (2006) 130.
65. R. Fuchs-Godec, *Colloids Surf. A*. 280 (2006) 130

66. R. Fuchus-Godec and G. Zerjav, *Corrosion Science*, 97 (2015) 7-16.
67. F. Bentiss, M. Traisnel, and M. Lagrenee, *Corros Sci*, 42 (2000) 127.
68. F. Zulkifli, N. Ali, M. S. M. Yusof, W. M. Khairul, R. Rahamathullah, M. I. N. Isa, and W. B. W. Nik, *Advances in Physical Chemistry* 2017, DOI: 10.1155/2017/8521623.
69. J. W. Wong, K. Hashimoto, and T. Shibamoto, *J Agric Food Chem*, 43 (1995) 2707.
70. A. A. El Bedawey, E. H. Mansour, M. S. Zaky, and A. A. Hassan, *Food and Nutrition Sciences*, 2017, DOI: 10.4236/fns.2010.11002.
71. M. G. Valladares-Cisneros, A. Esquivel-Rojas, V. M. Salinas-Bravo, and J. G. Gonzalez-Rodríguez, *Int J Electrochem Sci*, 11 (2016) 8067.
72. P. Muthukrishnan, P. Prakash, B. Jeyaprabha, and K. Shankar, *Arab J Chem*, 2015, DOI: 10.1016/j.arabjc.2015.09.005.
73. M. Prabakaran, S. H. Kim, A. Sasireka, V. Hemapriya, and I. M. Chung, *New J Chem*, 41 (2017) 3900.
74. H. Bendaha, H. Elmsellem, A. Aouniti, M. Mimouni, A. Chetouani, and B. Hammouti, *Mater Sci*, 52 (2016) 123.
75. L. Bammou, M. Belkhaouda, R. Salghi, O. Benali, A. Zarrouk, H. Zarrok, and B. Hammouti, *JAAUBAS*, 16 (2014) 83.
76. I. Hamdani, E. El Ouariachi, O. Mokhtari, A. Salhi, N. Chahboun, B. ElMahi, A. Bouyanzer, A. Zarrouk, B. Hammouti, and J. Costa, *Der Pharma Chemica*, 7 (2015) 252.
77. R. Salghi, D. B. Hmamou, O. Benali, S. Jodeh, I. Warad, O. Hamed, E. E. Ebenso, A. Oukacha, S. Tahrouch, and B. Hammouti, *In. J Electrochem Sci*, 10 (2015) 8403.
78. A. Garaya, W. Dhifi, M. Nehiri, A. Echchelh, M. Ebntouhami, A. Chaouch, W. Mnif, R. B. Chaouacha-Chekir, *Agri & BioTech*, 30 (2016) 1719.
79. K. Dahmani, M. Galai, M. Cherkaoui, A. El hasnaoui, and A. El Hessni, *JMES*, 8 (2017) 1676.
80. W. F. Smith, J. Hashemi, *Fundamentos de la ciencia e ingeniería de materiales*, (2006) The McGraw-Hill. U.S.A.
81. I. Raskin, D. M. Ribnicky, S. Komarnytsky, N. Ilic, A. Poulev, N. Borisjuk, and B. Fridlender, *Trends Biotechnol*, 20 (2002) 522.
82. C. W. Fennell, K. L. Lindsey, L. J. McGaw, S. G. Sparg, G. I. Stafford, E. E. Elgorashi, and J. Van Staden, *J Ethnopharm* 94 (2004) 205.
83. L. C. Fernández Linares, N. G. Rojas Avelizapa, T. G. Roldán Carrillo, M. E., Ramírez Islas, H. G. Zegarra Martínez, R. Uribe Hernández, R. J. Reyes Ávila, D. Flores Hernández, and J. M. Arce Ortega, *Manual de Técnicas de análisis de suelos aplicadas a la remediación de sitios contaminados*. Instituto Mexicano del Petróleo, Secretaría de Medio Ambiente y Recursos Naturales Instituto Nacional de Ecología. Mexico, 2006.